



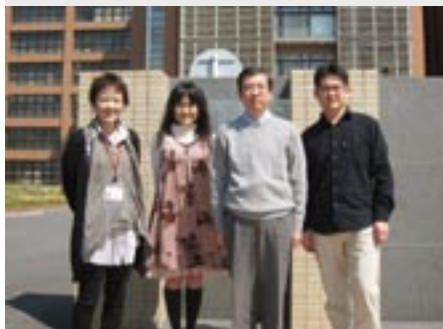
RESEARCH ACTIVITIES

Life and Coordination-Complex Molecular Science

Department of Life and Coordination-Complex Molecular Science is composed of four divisions of Biomolecular science, two divisions of Coordination molecular science and two adjunct divisions. Biomolecular science divisions cover the studies on the elucidation of functions and mechanisms for various types of sensor proteins, protein folding, molecular chaperone, and metal proteins. Coordination complex divisions aim to develop molecular catalysts for the transformation of organic molecules, activation small inorganic molecules, and reversible conversion between chemical and electrical energies. Interdisciplinary alliances in the Department aim to create new basic concepts for the molecular and energy conversion through the fundamental science conducted at each division.

Bioinorganic Chemistry of Metal-Containing Sensor Proteins

Department of Life and Coordination-Complex Molecular Science
Division of Biomolecular Functions



AONO, Shigetoshi
YOSHIOKA, Shiro
ISHIKAWA, Haruto
SAWAI, Hitomi

TANIZAWA, Misako

Professor
Assistant Professor
IMS Research Assistant Professor*
JSPS Post-Doctoral Fellow (–March '10)
Post-Doctoral Fellow (–April '10)
IMS Research Assistant Professor (May '10–)
Secretary

Hemeproteins are a typical metalloprotein, which show a variety of functions including oxygen storage/transport, electron transfer, redox catalysis with various substrates. Besides these traditional functions of hemeproteins, a new function of hemeprotein has been found recently, which is a sensor of diatomic gas molecules or redox change.¹⁾ In these heme-based sensor proteins, the heme acts as the active site for sensing the external signal such as gas molecules and redox change. Our research interests are focused on the elucidation of the structure-function relationships of these heme-based sensor proteins. We are also studying about an iron-sulfur (Fe-S) cluster-containing sensor protein responsible for the transcriptional regulation of nitrogenase gene.

1. Oxygen Sensor Proteins Responsible for Aerotaxis (Chemotaxis toward Molecular Oxygen) Control in Bacteria

Chemotaxis is a major biological signal transduction system, which consists of signal transducer proteins and several chemotaxis proteins including CheA, CheY, and CheW responsible for intermolecular signal transduction to control direction of flagellar rotation. Signal transducer proteins, sometimes called as MCPs (methyl-accepting chemotaxis proteins), bind a repellent or attractant in their sensor domain. Many chemical and physical stimuli act as a repellent or attractant, among which molecular oxygen is a typical gaseous signaling molecule. In this work, we have studied the structure and function relationships of MCPs, Aer2 and HemAT, that sense molecular oxygen for aerotaxis (chemotaxis toward molecular oxygen) control.

HemAT is well known as a MCP that senses molecular oxygen for aerotaxis control, which contains a *b*-type heme as the active site for sensing molecular oxygen. Though both of HemAT and Aer2 use a heme as the active site for sensing

molecular oxygen, the sensor domains of HemAT and Aer2 are different. HemAT and Aer2 adopt a globin domain and PAS domain as their sensor domains, respectively. Though the globin domain of HemAT shows a structural homology to myoglobin, it has a different heme environmental structure in the distal heme pocket from myoglobin. In the case of myoglobin, a distal His forms a hydrogen bond with the heme-bound oxygen to stabilize the heme-oxygen complex. However, there is no distal His in HemAT, in which a Thr is involved in the formation of a hydrogen bonding network upon oxygen binding to HemAT. We have studied conformational changes induced by oxygen binding by means of resonance Raman spectroscopy.

Aer2 is a new MCP responsible for aerotaxis of *Pseudomonas aeruginosa*, which adopts a PAS domain as a sensor domain. We have constructed an expression system of Aer2 in *E. coli* and purified the recombinant protein. The purified Aer2 shows the Soret, α and β peaks at 419, 578, and 543 nm, respectively, as shown in Figure 1. When the purified Aer2 is

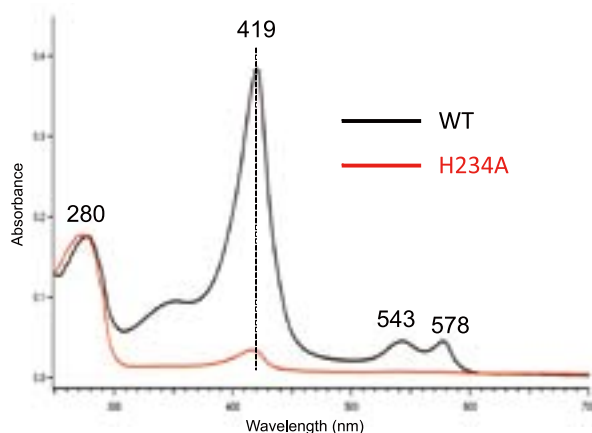


Figure 1. Electronic absorption spectra of wild-type and H234A mutant Aer2.

reacted with CO, CO-bound Aer2 is formed. The purified Aer2 shows a typical Resonance Raman spectrum of oxygen-bound heme proteins. These results indicate that Aer2 is purified as an oxygen-bound form.

Domain analysis by using SMART program (<http://smart.embl-heidelberg.de/>) reveals that Aer2 consists of a PAS domain in its N-terminal region. PAS domain is widely used as a sensor domain sensing various chemical and physical signals. PAS domains show a similar 3D structure, though their amino acid sequences do not necessarily show a high homology. Figure 2 shows X-ray crystal structures of the heme-containing PAS domain of FixL that is an oxygen sensor protein in FixL/FisJ two-component system. The PAS domain of Aer2 would

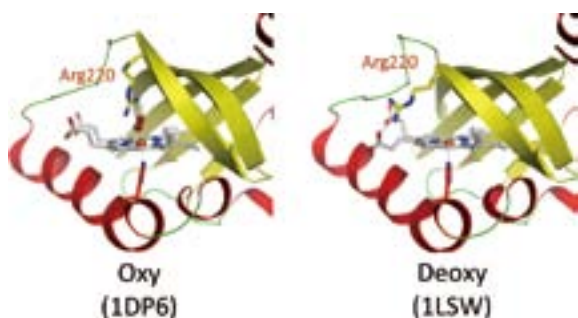


Figure 2. X-ray crystal structure of the PAS domain of FixL in oxy- and deoxy-forms. PDB accession numbers are shown in parenthesis.

be similar to that of FixL. Amino acid sequence alignments among heme-containing PAS domains including Aer2 show that a His residue is conserved at the position of 234 in Aer2, at which the proximal ligand of the heme is located in other heme-containing PAS domains. Site-directed mutagenesis reveals that His234 is indeed the proximal ligand of the heme in Aer2. Mutation of His234 to Ala results in loss of heme (Figure 1). Further characterization of Aer2 is now in progress.

2. The Role of the Fe-S Cluster in the Sensory Domain of Nitrogenase Transcriptional Activator VnfA from *Azotobacter vinelandii*²⁾

Transcriptional activator VnfA is required for the expres-

sion of the second nitrogenase system encoded in the *vnfH* and *vnfDGK* operons in *Azotobacter vinelandii*. VnfA belongs to a σ^N -dependent regulatory protein generally consisting of three major domains, and contains a GAF domain in its N-terminal region as a sensory domain. VnfA has a characteristic Cys-rich motif, Cys-X-Cys-XXXX-Cys, in its GAF domain. Although this motif is supposed to be a metal ions/cluster binding motif, metal ions/cluster in VnfA is not characterized yet. In the present study, we have purified full-length VnfA produced in *E. coli* as recombinant proteins (*Strep*-tag attached and tag-less proteins), enabling detailed characterization of VnfA for the first time. The EPR spectra of whole cells producing tag-less VnfA (VnfA) show distinctive signals assignable to a 3Fe-4S cluster in the oxidized form ($[\text{Fe}_3\text{S}_4]^+$). Although aerobically purified VnfA shows no vestiges of any Fe-S clusters, enzymatic reconstitution under anaerobic conditions reproduced $[\text{Fe}_3\text{S}_4]^+$ dominantly in the protein. Additional spectroscopic evidence of $[\text{Fe}_3\text{S}_4]^+$ *in vitro* is provided by anaerobically purified *Strep*-tag attached VnfA. Thus, spectroscopic studies both *in vivo* and *in vitro* indicate the involvement of $[\text{Fe}_3\text{S}_4]^+$ as a prosthetic group in VnfA. Molecular mass analyses reveal that VnfA is a tetramer both in the presence and absence of the Fe-S cluster. Quantitative data of iron and acid-labile sulfur in reconstituted VnfA are fitted with four 3Fe-4S clusters per a tetramer, suggesting that one subunit bears one cluster. *In vivo* β -gal assays reveal that the Fe-S cluster which is presumably anchored in the GAF domain by the N-terminal cysteine residues is essential for VnfA to exert its transcription activity on the target nitrogenase genes. Unlike the NifAL system of *A. vinelandii*, O_2 shows no effect on the transcriptional activity of VnfA but reactive oxygen species is reactive to cause disassembly of the Fe-S cluster and turns active VnfA inactive.

References

- 1) S. Aono, *Dalton Trans.* 3125–3248 (2008).
- 2) H. Nakajima, N. Takatani, K. Yoshimitsu, M. Itoh, S. Aono, Y. Takahashi and Y. Watanabe, *FEBS J.* **277**, 817–832 (2010).

* Present Address: Department of Chemistry, Graduate School of Science, Osaka University, Toyonaka, Osaka 560-0043

Elucidation of the Molecular Mechanisms of Protein Folding

Department of Life and Coordination-Complex Molecular Science
Division of Biomolecular Functions



KUWAJIMA, Kunihiro	Professor
MAKABE, Koki	Assistant Professor
NAKAMURA, Takashi	IMS Research Assistant Professor
CHEN, Jin	OIB Research Assistant Professor
TAKENAKA, Toshio	Post-Doctoral Fellow
TAKAHASHI, Kazunobu	Graduate Student*
MIZUKI, Hiroko	Technical Fellow
TANAKA, Kei	Secretary

Kuwajima group is studying mechanisms of *in vitro* protein folding and mechanisms of molecular chaperone function. Our goals are to elucidate the physical principles by which a protein organizes its specific native structure from the amino acid sequence. In this year, we carried out comparative studies of folding pathways of highly homologous proteins, goat α -lactalbumin and canine milk lysozyme.

1. Different Folding Pathways Taken by Highly Homologous Proteins, Goat α -Lactalbumin and Canine Milk Lysozyme¹⁾

Is the folding pathway conserved in homologous proteins? To address this question, we compared the folding pathways of goat α -lactalbumin and canine milk lysozyme using equilibrium and kinetic circular dichroism spectroscopy. Both Ca^{2+} -binding proteins have 41% sequence identity and essentially identical backbone structures. The Φ -value analysis, based on the effect of Ca^{2+} on the folding kinetics, showed that the Ca^{2+} -binding site was well organized in the transition state in α -lactalbumin, although it was not yet organized in lysozyme. Equilibrium unfolding and hydrogen-exchange 2D NMR analysis of the molten globule intermediate also showed that different regions were stabilized in the two proteins. In α -lactalbumin, the Ca^{2+} -binding site and the C-helix were weakly organized, whereas the A- and B-helices, both distant from the Ca^{2+} -binding site, were well organized in lysozyme. The results thus provide an example of highly homologous proteins taking different folding pathways. To understand the molecular origin of this difference, we investigated the native three-dimensional structures of the proteins in terms of non-local

contact clusters, a parameter based on the residue–residue contact map and known to be well correlated with the folding rate of non-two-state proteins. There were remarkable differences between the proteins in the distribution of the non-local contact clusters, and these differences provided a reasonable explanation of the observed difference in the folding initiation sites. In conclusion, the protein folding pathway is determined not only by the backbone topology but also by the specific side-chain interactions of contacting residues.

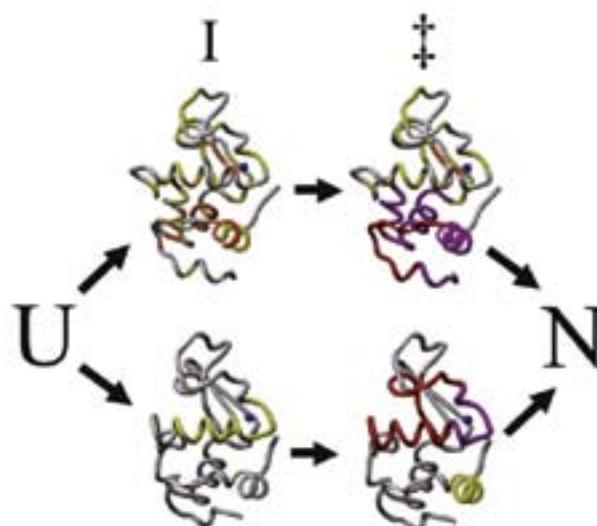


Figure 1. A folding model of α -lactalbumin/lysozyme family proteins. Two parallel pathways are available for the backbone topology of this family, and the lower and upper pathways are taken by goat α -lactalbumin and canine milk lysozyme, respectively, because of the distributions of the strong clusters in their native 3D structures.

2. Flexible Recognition of the tRNA G18 Methylation Target Site by TrmH Methyltransferase through First Binding and Induced Fit Processes²⁾

Transfer RNA (Gm18) methyltransferase (TrmH) catalyzes methyl transfer from S-adenosyl-L-methionine to a conserved G18 in tRNA. We investigated the recognition mechanism of *Thermus thermophilus* TrmH for its guanosine target. Thirteen yeast tRNA(Phe) mutant transcripts were prepared in which the modification site and/or other nucleotides in the D-loop were substituted by dG, inosine, or other nucleotides. We then conducted methyl transfer kinetic studies, gel shift assays, and inhibition experiments using these tRNA variants. Sites of methylation were confirmed with RNA sequencing or primer extension. Although the G18G19 sequence is not essential for methylation by TrmH, disruption of G18G19 severely reduces the efficiency of methyl transfer. There is strict recognition of guanosine by TrmH, in that methylation occurs at the adjacent G19 when the G18 is replaced by dG or adenosine. The fact that TrmH methylates guanosine in D-loops from 4 to 12 nucleotides in length suggests that selection of the position of guanosine within the D-loop is relatively flexible. Our studies also demonstrate that the oxygen 6 atom of the guanine base is a positive determinant for TrmH recognition. The recognition process of TrmH for substrate is inducible and product-inhibited, in that tRNAs containing Gm18 are excluded by TrmH. In contrast, substitution of G18 with dG18 results in the formation of a more stable TrmH-tRNA complex. To address the mechanism, we performed the stopped-flow pre-steady state kinetic analysis. The result clearly showed that the binding of TrmH to tRNA is composed of at least three steps, the first bi-molecular binding and the subsequent two uni-molecular induced-fit processes.

3. Adaptation of a Hyperthermophilic Group II Chaperonin to Relatively Moderate Temperatures³⁾

Group II chaperonins exist in archaea and the eukaryotic

cytosol, and mediate protein folding in an ATP-dependent manner. We have been studying the reaction mechanism of group II chaperonins using alpha chaperonin, the recombinant chaperonin alpha subunit homo-oligomer from a hyperthermophilic archaeon, *Thermococcus* sp. strain KS-1 (*T. KS-1*). Although the high stability and activity of *T. KS-1* alpha chaperonin provided advantages for our study, its high thermophilicity caused the difficulty in using various analytical methods. To resolve this problem, we tried to adapt *T. KS-1* alpha chaperonin to moderate temperatures by mutations. The comparison of amino acid sequences between 26 thermophilic and 17 mesophilic chaperonins showed that three amino acid replacements are likely responsible for the difference of their optimal temperatures. We introduced three single mutations and also their double combinations into *T. KS-1* alpha chaperonin. Among them, K323R single mutant exhibited the improvements of the folding activity and the ATP-dependent conformational change ability at lower temperatures, such as 50 °C and 40 °C. Since K323 may secure helix 12 in the closed conformation by interacting with D198, the replacement of Lys to Arg likely induced the higher mobility of the built-in lid, resulting in the higher activity at relatively low temperatures.

References

- 1) T. Nakamura, K. Makabe, K. Tomoyori, K. Maki, A. Mukaiyama and K. Kuwajima, *J. Mol. Biol.* **396**, 1361–1378 (2010).
- 2) A. Ochi, K. Makabe, K. Kuwajima and H. Hori, *J. Biol. Chem.* **285**, 9018–9029 (2010).
- 3) T. Kanzaki, S. Ushioku, A. Nakagawa, T. Oka, K. Takahashi, T. Nakamura, K. Kuwajima, A. Yamagishi and M. Yohda, *Protein Eng., Des. Sel.* **23**, 393–402 (2010).

* carrying out graduate research on Cooperative Education Program of IMS with the University of Tokyo

Elucidation of Dynamical Structures of Biomolecules toward Understanding the Mechanisms Underlying Their Functions

Department of Life and Coordination-Complex Molecular Science
Division of Biomolecular Functions



KATO, Koichi
YAMAGUCHI, Takumi
KAMIYA, Yukiko
UEKUSA, Yoshinori
SERVE, Olivier
MONDAL, Gautam
CHOO, Yeun-Mun
SUGIHARA, Takahiro
YAGI-UTSUMI, Maho
NISHIO, Miho
YOSHIKAWA, Sumi
HIRANO, Takashi
BUNKO, Yuji
UNO, Tsuyoshi
YAMAMOTO, Sayoko
SUZUKI, Mariko
ISONO, Yukiko
TANAKA, Kei

Professor
Assistant Professor
IMS Research Assistant Professor
JSPS Post-Doctoral Fellow
Post-Doctoral Fellow
Visiting Scientist
Visiting Scientist
Research Fellow
Research Fellow
Graduate Student*
Technical Fellow
Technical Fellow
Secretary

Our biomolecular studies are based on detailed analyses of structures and dynamics of various biological macromolecules and their complexes at atomic level, primarily using nuclear magnetic resonance (NMR) spectroscopy. In particular, we conducted studies aimed at elucidating dynamic structures of glycoconjugates and proteins for integrative understanding of the mechanisms underlying their biological functions. For this purpose, we use multidisciplinary approaches integrating the methodologies of molecular and cellular biology and nano-science along with molecular spectroscopy.

1. NMR Characterization of the Interaction between Amyloid β -Peptide and Ganglioside Clusters^{1,2)}

Gangliosides are targets for a variety of pathologically relevant proteins, including amyloid β ($A\beta$), an important component implicated in Alzheimer's disease (AD). To provide a structural basis for this pathogenic interaction associated with AD, we conducted NMR analyses of the interactions of $A\beta$ with gangliosides using lyso-GM1 micelles as a model system. Our NMR data revealed that the sugar-lipid interface is primarily perturbed upon binding of $A\beta$ to the micelles, underscoring the importance of the inner part of the ganglioside cluster for accommodating $A\beta$ in comparison with the outer carbohydrate branches that provide microbial toxin- and virus-binding sites. To provide a more detailed understanding of the interaction mode of $A\beta$ and gangliosides, we observed NMR peaks originating from isotopically labeled $A\beta$ bound to the micelles. The secondary chemical shifts of the polypeptide backbone indicated that $A\beta$ forms discontinuous α -helices upon binding to the gangliosidic micelles, leaving the remaining regions disordered. TROSY-based saturation transfer

analyses revealed that $A\beta$ lies on hydrophobic/hydrophilic interface of the ganglioside cluster exhibiting an up-and-down topological mode in which the two α -helices and the C-terminal dipeptide segment are in contact with the hydrophobic interior, whereas the remaining regions are exposed to the aqueous environment (Figure 1). These findings suggest that the ganglioside clusters provide a unique platform at their hydrophobic/hydrophilic interface for binding coupled with conformational transition of $A\beta$ molecules, rendering their spatial rearrangements restricted to promote specific inter-molecular interactions.

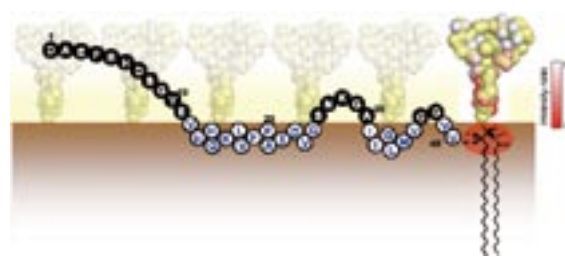


Figure 1. Schematic drawing of $A\beta(1-40)$ lying on the hydrophobic/hydrophilic interface of ganglioside clusters. The amino acid residues exposed to the hydrophilic and hydrophobic milieus are represented by closed and open circles with single-letter codes. The sugar hydrogen atoms coloured in red and the ceramide hydrogen atoms located within the red ellipse area exhibit lower peak intensity ratios, indicating that they are in close spatial proximity of the C-terminus of $A\beta(1-40)$.

2. Structural Basis of the Protein-Fate Determination in Cells³⁻⁶⁾

In eukaryotic cells, folding of nascent proteins is assisted by complexes of molecular chaperones in the endoplasmic

reticulum (ER). Correctly folded proteins are transferred from the ER to the Golgi complex on the secretion pathway, while terminally misfolded proteins are transferred from the ER to the cytosol and subsequently degraded in the ubiquitin (Ub)- and proteasome-mediated proteolytic pathway. We conducted structural biology studies of the ER chaperones, the cargo receptors, and the ubiquitinating enzymes to elucidate the mechanisms underlying the protein-fate determination in cells.

Protein disulfide isomerase (PDI) is a major protein in the ER, operating as an essential folding catalyst and molecular chaperone for disulfide-containing proteins by catalyzing the formation, rearrangement, and breakage of their disulfide bridges. By combined use of NMR and small-angle X-ray scattering methods, we reveal the redox-dependent domain rearrangement of PDI coupled with exposure of its substrate-binding hydrophobic surface spanning the *b'* and *a'* domains (Figure 2A). On the basis of these data, we propose a mechanistic model of PDI action; the *a'* domain transfers its own disulfide bond into the unfolded protein accommodated on the hydrophobic surface, which consequently changes into a *closed* form releasing the oxidized substrate.

The intracellular lectin ERGIC-53 and the EF-hand Ca^{2+} -binding protein MCFD2, which have been identified as products of the causative genes of combined deficiency of coagulation factors V and VIII (F5F8D), form a complex operating as cargo receptor of these coagulation factors. We determined the 3D structure of ERGIC-53 complexed with MCFD2 by X-ray crystallographic analysis in conjunction with NMR and ultracentrifugation analyses (Figure 2B). The interaction is independent of sugarbinding of ERGIC-53 and involves most of the missense mutation sites of MCFD2 so far reported in F5F8D. Comparison with the previously reported uncomplexed structure of each protein indicates that MCFD2 but not ERGIC-53-CRD undergoes significant conformational alterations upon complex formation. These findings provide a structural basis for the cooperative interplay between ERGIC-53 and MCFD2 in capturing FV and FVIII.

A key question in ubiquitination is how E2-E3 complexes can deal with the various acceptor sites distributed on the substrate surface to perform multiple ubiquitination and/or poly-Ub elongation. We solved the crystal structure of an intermediate of the UbcH5b E2 enzyme conjugated with Ub which is assembled into an infinite spiral through the backside interaction (Figure 2C). This active complex may provide multiple E2 active sites, enabling efficient ubiquitination of substrates. Indeed, biochemical assays support a model in which the self-assembled UbcH5b~Ub can serve as a bridge for the gap between the lysine residue of the substrate and the catalytic cysteine of E2.

Award

YAGI-UTSUMI, Maho; Poster Presentation Award, The 74th Annual meeting in The Japanese Biochemical Society, Chubu Branch (2010).

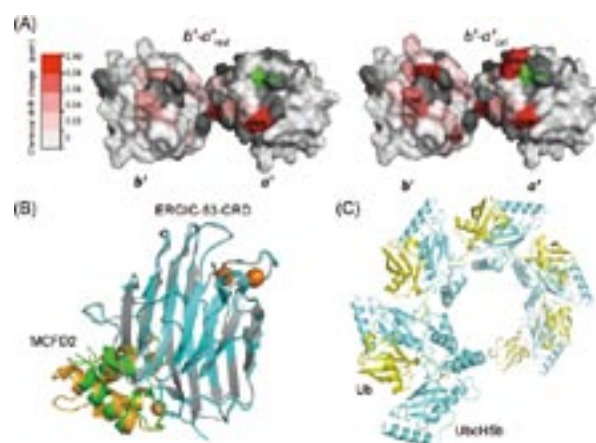


Figure 2. (A) Mapping on the 3D model of *b'*-*a'* (reduced form) of the residues whose chemical shift were perturbed upon binding with mastoparan (as a model ligand) in the reduced (left) and oxidized (right) forms of *b'*-*a'*. Red gradient indicates the strength of the perturbation. The proline residues and the residues whose ¹H-¹⁵N HSQC peak could not be used as a probe due to broadening and/or overlapping are shown in gray. The catalytic cysteine residues appear in green. (B) 3D structures of MCFD2 and ERGIC-53-CRD. Uncomplexed structures of rat ERGIC-53 (cyan) and human MCFD2 (orange) are superimposed on our crystal structure of the complex between human ERGIC-53 (gray) and MCFD2 (green). The bound calcium ions are shown as spheres. (C) Formation of the self-assembly of the UbcH5b~Ub conjugate through the backside interaction.

References

- 1) M. Utsumi, Y. Yamaguchi, H. Sasakawa, N. Yamamoto, K. Yanagisawa and K. Kato, *Glycoconjugate J.* **26**, 999–1006 (2009).
- 2) M. Yagi-Utsumi, T. Kameda, Y. Yamaguchi and K. Kato, *FEBS Lett.* **584**, 831–836 (2010).
- 3) E. Sakata, T. Satoh, S. Yamamoto, Y. Yamaguchi, M. Yagi-Utsumi, E. Kurimoto, K. Tanaka, S. Wakatsuki and K. Kato, *Structure* **18**, 138–147 (2010).
- 4) O. Serve, Y. Kamiya, A. Maeno, M. Nakano, C. Murakami, H. Sasakawa, Y. Yamaguchi, T. Harada, E. Kurimoto, M. Yagi-Utsumi, T. Iguchi, K. Inaba, J. Kikuchi, O. Asami, T. Kajino, T. Oka, M. Nakasako and K. Kato, *J. Mol. Biol.* **396**, 361–374 (2010).
- 5) M. Nishio, Y. Kamiya, T. Mizushima, S. Wakatsuki, H. Sasakawa, K. Yamamoto, S. Uchiyama, M. Noda, A. R. McKay, K. Fukui, H.-P. Hauri and K. Kato, *Proc. Natl. Acad. Sci. U. S. A.* **107**, 4034–4039 (2010).
- 6) M. Nakasako, A. Maeno, E. Kurimoto, T. Harada, Y. Yamaguchi, T. Oka, Y. Takayama, A. Iwata and K. Kato, *Biochemistry* **49**, 6953–6962 (2010).

Structure-Function Relationship of Metalloproteins

Department of Life and Coordination-Complex Molecular Science
Division of Biomolecular Functions



FUJII, Hiroshi	Associate Professor
KURAHASHI, Takuya	Assistant Professor
CONG, Zhiqi	IMS Fellow
NAKAGAWA, Takafumi	Post-Doctoral Fellow
WANG, Shunlan	Graduate Student
TANIZAWA, Misako	Secretary

Metalloproteins are a class of biologically important macromolecules, which have various functions such as oxygen transport, electron transfer, oxidation, and oxygenation. These diverse functions of metalloproteins have been thought to depend on the ligands from amino acid, coordination structures, and protein structures in immediate vicinity of metal ions. In this project, we are studying the relationship between the electronic structures of the metal active sites and reactivity of metalloproteins.

1. Unique Property and Reactivity of High-Valent Manganese-Oxo versus Manganese-Hydroxo in the Salen Platform^{1,2)}

To gain an understanding of oxidation reactions by Mn^{III}(salen), a reaction of Mn^{III}(salen) with *m*-chloroperoxybenzoic acid in the absence of a substrate is investigated. UV-vis, perpendicular- and parallel-mode electron paramagnetic resonance and X-ray absorption spectroscopy show the resulting solution contains Mn^{IV}(salen)(O) as a major product and Mn^{IV}(salen)(OH) as a minor product. Mn^{IV}(salen)(O) readily reacts with 4-H-2,6-*tert*-Bu₂C₆H₂OH (BDE_{OH} = 82.8 kcal/mol), 4-CH₃CO-2,6-*tert*-Bu₂C₆H₂OH (BDE_{OH} = 83.1 kcal/mol) and 4-NC-2,6-*tert*-Bu₂C₆H₂OH (BDE_{OH} = 84.2 kcal/mol) at 203 K, following second-order rate kinetics (BDE_{OH}; homolytic bond dissociation energy of an OH bond). Mn^{IV}(salen)(OH) reacts with 4-CH₃CO-2,6-*tert*-Bu₂C₆H₂OH (BDE_{OH} = 83.1 kcal/mol) much more slowly under the identical conditions than Mn^{IV}(salen)(O), and does not react with 4-NC-2,6-*tert*-Bu₂C₆H₂OH (BDE_{OH} = 84.2 kcal/mol), suggesting thermodynamic hydrogen-atom abstracting ability of Mn^{IV}(salen)(OH) is about 83 kcal/mol. The rate constant for reactions of Mn^{IV}(salen)(OH) with phenols are not dependent on

the concentration of phenols, suggesting that Mn^{IV}(salen)(OH) might bind phenols prior to the rate-limiting oxidation reactions. Quantum chemical calculations are carried out for Mn^{IV}(salen)(O) and Mn^{IV}(salen)(OH), both of which well reproduce the EXAFS structures as well as the electronic configurations. It is also indicated that protonation of Mn^{IV}(salen)(OH) induces a drastic electronic structural change from Mn^{IV}-phenolate to Mn^{III}-phenoxyl radical, which is also consistent with the experimental observation.

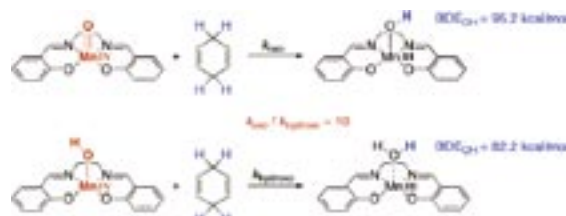


Figure 1. Hydrogen abstractions of oxo-manganese(IV) salen and hydroxy-manganese(IV) salen complexes.

2. Resonance Raman Study of a High-Valent Fe=O Porphyrin Complex as a Model for Peroxidase Compound II³⁾

Horseradish peroxidase (HRP) catalyzes the oxidation of organic substrates using H₂O₂ as a specific oxidant. Upon reaction with H₂O₂, HRP sequentially forms two reaction intermediates known as compound I and compound II, before returning to the original ferric state. Compound I and compound II are respectively 2 and 1 oxidative equivalents higher than the Fe^{III} state, and respectively correspond to the Fe^V and Fe^{IV} formal oxidation states. Compound II of HRP exhibits a ν_{Fe=O} resonance Raman (RR) band at 775 and 787 cm⁻¹ at pH

7 and 11, respectively. The 12 cm^{-1} upshift of the $\nu_{\text{Fe=O}}$ mode of HRP compound II upon alkalization is caused by elimination of the hydrogen bond between the oxygen atom and the distal His and is regarded as a “distal effect.” The $\nu_{\text{Fe=O}}$ mode of the Fe^{IV} state of myoglobin (Mb) at pH 8.5 is located at *ca.* 800 cm^{-1} (sperm whale Mb at 797 cm^{-1} and horse heart Mb at 804 cm^{-1}), where no hydrogen bond exists between the oxygen atom and the distal His. There is a 13 cm^{-1} frequency difference in the $\nu_{\text{Fe=O}}$ mode between HRP at 787 cm^{-1} and Mb at 800 cm^{-1} . This has been interpreted as a result of a “proximal effect.” Both HRP and Mb have a proximal His residue. However, the proximal His of HRP has the anionic character of imidazolate (Im^-), while the proximal His of Mb is considered to be neutral.

Many Fe=O porphyrin model complexes with 1-methylimidazole (1MeIm) or a solvent molecule acting as the axial ligand have been prepared and characterized by RR spectroscopy, in order to obtain insights into the electronic structures and reactivities of hemoproteins. However, there have been no reports of model complexes with Im^- as a *trans* axial ligand. In the present study, we have prepared an Fe=O porphyrin model complex with Im^- as the axial ligand and identified the $\nu_{\text{Fe=O}}$ mode at 792 cm^{-1} , which is significantly lower than that of an analogous complex with 1MeIm as the axial ligand (815 cm^{-1}). Thus, the imidazolate complex could be regarded as a model for compound II of HRP. The experimental details are described in Supporting Information.

3. Direct Probing of Spin State Dynamics Coupled with Electronic and Structural Modifications by Picosecond Time-Resolved XAFS⁴

Molecular magnetic systems such as nanomagnets and biological systems have attracted much interest in recent years. In disordered magnetic systems, where the spin system does not have macroscopic magnetization, it is crucial to directly observe the transient spin states to aid in the understanding and controlling of the dynamic magnetic properties. In studies of ultrafast spin dynamics, pico- and femtosecond time scales are now accessible with advanced optical pump-probe measurement using two ultrafast lasers. However, it is not trivial to deconvoluting the dynamics of the spin state from transient optical signal. Although the magneto-optical effect has been applied to macroscopic magnetization, it is difficult to apply in disordered magnetic systems. To overcome these difficulties, a pulsed hard X-ray has been utilized as a probe for the dynamics of the inner-atomic transitions.

The first direct observation of the transient spin-state in a disordered magnetic system with time-resolved XAFS is reported. By observing the evolution of the Fe^{II} $1s\text{--}3d$ transition, the spin crossover transition from the 1A_1 low spin state to 5T_2 high spin state has been directly observed on a picos-

econd time scale. Moreover, observation of the transient spin state with time-resolved XAFS allows for the investigation of the variations in the electronic state and molecular structure. This unique experimental technique probes the excited states involved in the ultrafast photoinduced reactions in disordered magnetic systems.

4. Paramagnetic ^{13}C and ^{15}N NMR Analyses of the Push- and Pull-Effects in Cytochrome *c* Peroxidase and *Coprinus cinereus* Peroxidase Variants: Functional Roles of Highly-Conserved Amino Acids around Heme⁵

Paramagnetic ^{13}C and ^{15}N nuclear magnetic resonance (NMR) spectroscopy of heme-bound cyanide ($^{13}\text{C}^{15}\text{N}$) was applied to 11 cytochrome *c* peroxidase (CcP) and *Coprinus cinereus* peroxidase (CIP) mutants to investigate contributions to the push- and pull-effects of conserved amino acids around heme. The ^{13}C and ^{15}N NMR data for the distal His and Arg mutants indicated that distal His is the key amino acid residue creating the strong pull-effect and that distal Arg assists. The mutation of distal Trp of CcP to Phe, the amino acid at this position in CIP, changed the push- and pull-effects close to those of CIP, whereas the mutation of distal Phe of CIP to Trp changed this mutant to become CcP-like. The ^{13}C NMR shifts for the proximal Asp mutants clearly showed that the proximal Asp-His hydrogen-bonding increase the push-effect. However, even in absence of a hydrogen-bond the push-effect of proximal His in peroxidase is significantly stronger than in globins. Comparison of the present NMR data with the compound I formation rate constants and crystal structures of these mutants showed that (1) the base catalysis of the distal His is more critical for rapid compound I formation than its acid catalysis, (2) the primary function of the distal Arg is to maintain the distal heme pocket in favor of rapid compound I formation via hydrogen-bonding, and (3) the push-effect is the major contributor to the differential rates of compound I formation in wild-type peroxidases.

References

- 1) T. Kurahashi, M. Hada and H. Fujii, *J. Am. Chem. Soc.* **131**, 12394–12405 (2009).
- 2) T. Kurahashi, A. Kikuchi, Y. Shiro, M. Hada and H. Fujii, *Inorg. Chem.* **49**, 6664–6672 (2010).
- 3) H. Ishimaru, H. Fujii and T. Ogura, *Chem. Lett.* **39**, 332–333 (2010).
- 4) S. Nozawa, T. Sato, M. Chollet, K. Ichyanagi, A. Tomita, H. Fujii, S. Adachi and S. Koshihara, *J. Am. Chem. Soc.* **132**, 61–63 (2010).
- 5) D. Nonaka, H. Wariishi and H. Fujii, *Biochemistry* **49**, 49–57 (2010).

Fabrication of Silicon-Based Planar Ion-Channel Biosensors and Integration of Functional Cell Membrane Model Systems on Solid Substrates

Department of Life and Coordination-Complex Molecular Science
Division of Biomolecular Sensing



URISU, Tsuneo
TERO, Ryugo
WANG, Zhihong
RAHMAN, Mashuur
ASANO, Toshifumi
NAGAIHIRO, Takeshi
NAGAOKA, Yasutaka
UNO, Hidetaka
NAKAI, Naohito
SHANG, Zhi-Guo
FUJIWARA, Kuniyo
SHIMIZU, Atsuko

Professor
Assistant Professor
Post-Doctoral Fellow
Post-Doctoral Fellow
Post-Doctoral Fellow
Post-Doctoral Fellow
Research Fellow
Graduate Student
Graduate Student
Graduate Student
Graduate Student
Secretary

We are interested in the investigation of cell membrane surface reactions and the pathogen mechanism of the neurodegenerative diseases, based on the molecular science. We are advancing two subjects, aiming the creation and development of new molecular science field, “medical molecular science.” One is the development of ion channel biosensor and its application to the neural network analyzer device. The other is the fundamental understanding of bilayer membrane properties using the artificial lipid bilayers on solid substrates, which is called supported bilayers, by means of atomic force microscope and fluorescence microscope-based techniques.

1. Development of Neural Network Device and Precise Microfabrications

We have successfully developed the neural cell device which emits the action potential by the photo-stimulation using a photo-receptor ion channel protein and the ion channel biosensor as the detector of the action potential. As an application of these elementary devices, we are now developing the neural cell network devices, using the state-of-the-art precision work combining the superprecision machining, the hot emboss technology, and the LIGA process. The high precision fabri-

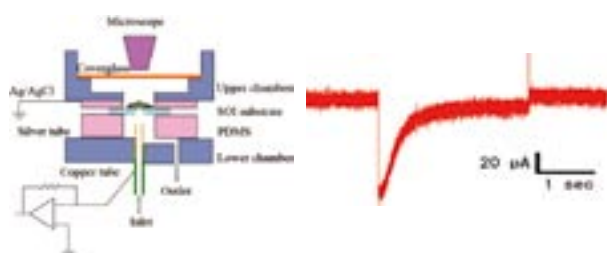


Figure 1. Structure of ion channel biosensor, and the observed channel current gated by laser irradiation. Chr2 is expressed on the C2C12 cell set on the biosensor substrate.

cation technology will bring a significant breakthrough into the brain science.

2. Surface-Induced Phase Separation of Sphingomyelin/Cholesterol/Ganglioside GM1-Planar Bilayer on Mica Surfaces and Microdomain Molecular Conformation that Accelerates A β Oligomerization

Ganglioside GM1 mediates the amyloid beta (A β) aggregation that is the hallmark of Alzheimer’s disease (AD). To investigate how ganglioside-containing lipid bilayers interact with A β , we examined the interaction between A β 40 and supported planar lipid bilayers (SPBs) on mica and SiO₂ substrates using atomic force microscopy, fluorescence microscopy, and molecular dynamics computer simulations. These SPBs contained several compositions of sphingomyelin, cholesterol, and GM1 which covers compositions commonly seen in eukaryotic biomembranes and were treated at physiological salt concentrations. Surprisingly high speed A β aggregations of fibril formation were induced for all GM1 concentrations examined on the mica surface, but only globular agglomerates are formed slowly on the SiO₂ surfaces. Especially for the 20 mol% GM1 concentration on the mica surface, unique triangular domains were formed and the high speed A β aggregations were observed only outside of the triangular domains. We have found that some unique surface-induced phase separations are induced due to the GM1 clustering effects and the strong interactions between the GM1 head group and the water layer adsorbed in the ditrigonal cavities on the mica surface. The speed of A β 40 aggregation and the shape of the agglomerates depend on the molecular conformation of GM1, which varies depending on the substrate materials. We identified the conformation that significantly accelerates A β 40 aggregation, and we think that the detailed knowledge about the GM1 molecular

conformation obtained in this work will be useful to those investigating A β -GM1 interactions.¹⁾

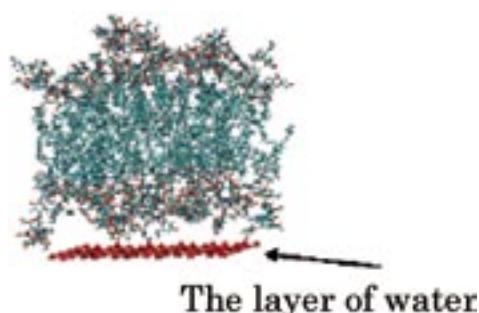


Figure 2. Starting model of the calculation, including the substrate effects. CHOL/GM1 (50:50)-SPB sitting on a layer of water molecules trapped in the ditrigonal cavities with 0.52-nm spacing of the mica surface.

3. Clustering Effects of GM1 and Formation Mechanisms of Interdigitated Liquid Disordered Domains in GM1/SM/CHOL-Supported Planar Bilayers on Mica Surface

We investigate the formation mechanisms of the interdigitated liquid disordered domain (ILDD), which is observed in the ganglioside (GM1)/sphingomyelin (SM)/cholesterol (CHOL) bilayers on a mica surface and accelerates the formation of fibrillar A β agglomerates, using molecular dynamics computer simulations and atomic force microscopy. The ILDD structure is stable both on mica and SiO₂ surfaces, but it is observed only on the mica surface. We conclude that the phase separation of SM- and GM1-rich domains is induced by GM1 clustering and the interaction between the GM1 head group and the water layer adsorbed in the ditrigonal cavity on the mica surface.

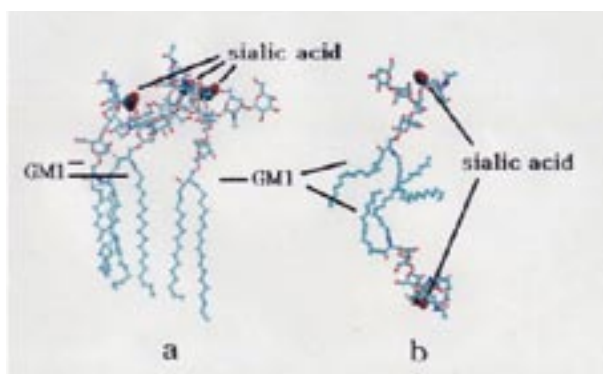


Figure 3. Molecular structures of GM1 and SM in the lipid bilayer of GM1_x/SM_{32-x}/CHOL₃₂ on the mica surface, for $x = 16$ (a) and 24 (b) after 10-ns simulation.

4. Anomalous Diffusion in Supported Lipid Bilayers Induced by Nanostructures on Substrate Surfaces

Lateral organization and diffusion of lipids and membrane proteins are crucial factors of biological reactions on cell membranes such as signal transduction and cell recognition. We have observed directly the lipid diffusion in supported lipid bilayers (SLBs) by single molecule tracking (SMT) method. SMT measurement of fluorescent dye-labeled lipid (lissamine rhodamine B labeled dipalmitoyl-phosphatidylethanolamine; Rb-DPPE, $E_x/E_m = 557 \text{ nm}/571 \text{ nm}$) in dioleoylphosphatidylcholine (DOPC)-SLBs on thermally oxidized SiO₂/Si(100) and step-and-terrace TiO₂(100) surfaces was performed by diagonal illumination method applying an objective type total internal reflection fluorescence microscope. The SiO₂ surface has amorphous structure of $\sim 1 \text{ nm}$ at peak-to-valley. The step-and-terrace TiO₂(100) surface has linear atomic steps at 550 nm interval, and 50–300 nm oval pits surrounded by an atomic step exists in terraces. Diffusion of Rb-DPPE in the DOPC-SLBs on SiO₂/Si(100) and TiO₂(100) surfaces were recorded at the time resolution ranging from 497 μs (2011 fps) to 30 ms (33 fps), and the diffusion coefficients on various time scale were evaluated from the time evolution of mean square displacement ($\langle r^2 \rangle$). The diffusion coefficients (D) of Rb-DPPE decreased with diffusion length, and their tendency depend on the substrate nanostructures (Figure 4). On TiO₂(100) decrease in diffusion coefficient (D) is observed at the mean diffusion distance ($\sqrt{\langle r^2 \rangle}$) less than 400 nm, which corresponds to the interval of the atomic steps. We attribute this anomalous diffusion to the surface atomic steps on the TiO₂(100) surface.

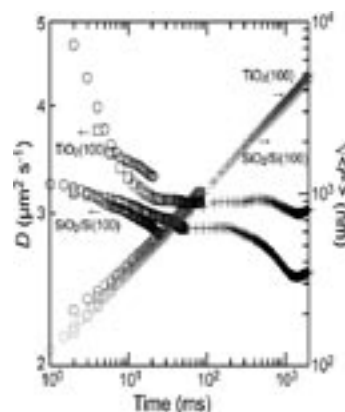


Figure 4. Time dependence of the diffusion coefficients (D) of Rb-DPPE and the mean diffusion distance ($\sqrt{\langle r^2 \rangle}$).

Reference

- 1) Y.-Li. Mao, Z.-G. Shang, Y. Imai, T. Hoshino, R. Tero, M. Tanaka, N. Yamamoto, K. Yanagisawa and T. Urisu, *Biochim. Biophys. Acta, Biomemb.* **1798**, 1090–1099 (2010).

Awards

TERO, Ryugo; CSJ Presentation Award 2010.

UNO, Hidetaka; 3rd International Symposium of Nano-medicine, Young Scientist Award.

Investigation of Molecular Mechanisms of Transporters and Receptors in Membrane by Using Stimulus-Induced Difference FT-IR Spectroscopy

Department of Life and Coordination-Complex Molecular Science
Division of Biomolecular Sensing



FURUTANI, Yuji
KIMURA, Tetsunari
GUO, Hao
SHIMIZU, Atsuko

Associate Professor
Assistant Professor
Graduate Student
Secretary

Membrane proteins are important for homeostasis of living cells, which work as ion channel, ion pump, various types of chemical and biophysical sensors, and so on. These proteins are considered as one of important targets for biophysical studies. However, their molecular mechanisms have not been studied well, because X-ray crystallography and NMR spectroscopy are hard to access them in general.

Our main goal is to clarify molecular mechanisms of transporters and receptors in cell membrane mainly by using stimulus-induced difference infrared spectroscopy which is sensitive to the structural and environmental changes of organic and bio-molecules.

Our research group was launched in 2009 and has been setting up experimental equipments.

1. Time-Resolved FT-IR Spectroscopy Detecting O–H and O–D Stretching Vibrations of Light-Driven Proton and Chloride-Ion Pump Proteins

Bacteriorhodopsin (bR) is one of well known light-driven proton pump protein, which has an all-*trans* retinal as a chromophore. Upon the light absorption, photo-isomerization of the retinal occurs from the all-*trans* to 13-*cis* form in less than one picosecond, followed by a cyclic reaction that comprises a series of intermediates, called as the K, L, M, N, and O states, back to the bR ground state (BR).

Hydration level of bR film samples are optimized by dropping the deuterium glycerol/water drops (20% v/v) around the sample. This sample preparation allowed us to collect the accurate light-induced difference FT-IR spectra (3850 to 1000 cm^{-1}) including the X–H and X–D stretching regions, corresponding to the structural changes in the hydrophobic and hydrophilic parts, respectively. By analyzing these spectral

Time-resolved light-induced difference FT-IR spectroscopy in IMS

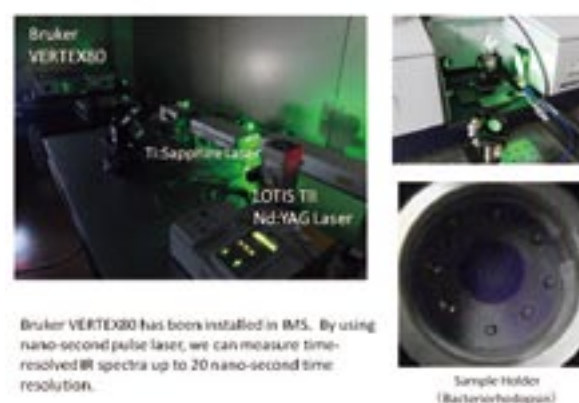


Figure 1. Light-induced difference FT-IR measurement system.

changes, real-time hydrogen-bonding changes of internal water molecules and protein moiety of BR will be elucidated, leading to better understand of the light-driven proton pumping mechanism of BR.

Dr. Kimura joined our group in Dec. 2009 and started to measure time-resolved infrared spectra of a light-driven chloride-ion pump, *pharaonis* halorhodopsin (*pHR*). The previous low-temperature FT-IR measurement revealed that the specific interaction among a chloride ion, the protonated Schiff base and internal water molecules changes upon the formation of K, L₁ and L₂ intermediates [Shibata *et al.*, *Biochemistry* **44**, 12279 (2005).] However, the structures in the later intermediates, such as N, O, and *pHR'* are still unclear. In this study, we applied time-resolved FT-IR difference spectroscopy on *pHR* at 12.5 μs time resolution. As a result, we found that the H/D unexchangeable X–H groups showed two negative peaks at 3289 and 3315 cm^{-1} in amide A region, with different decay kinetics. The former band was decayed with the time

constant of 4.2 ms, but the latter decay was fitted with the two time constants of 700 μ s and 6.2 ms. The faster and slower phases correspond to the conformational changes from L_2 to $[N \leftrightarrow O]$ states accompanying chloride release and from $[N \leftrightarrow O]$ to pHR' involving chloride uptake, respectively.

2. Perfusion-Induced Difference FT-IR Spectroscopy Investigating Ion Binding Sites of Membrane Proteins

Recently, it has been demonstrated that stimulus-induced attenuated total reflection (ATR) FT-IR spectroscopy is one of the promising techniques for the investigation of the molecular mechanism of membrane proteins.

ATR FT-IR spectroscopy is a useful technique to obtain infrared spectra of membrane proteins immersed in aqueous solution. By exchanging buffer with and without salts, the difference spectra between the two conditions provide the structural information relating to the interaction change between membrane proteins and ions, especially around the ion binding site. We first applied this technique to a component of a flagellar motor protein complex, PomA/PomB, which forms ion channels passing Na^+ ions to drive the rotation of flagella. We revealed that Asp24 is deprotonated upon binding of Na^+ ion to PomA/PomB and is involved in an Na^+ pathway, which probably reduces the energetic barrier formed in the inside of the hydrophobic channel.¹⁾

Application of this ATR FT-IR to other membrane proteins, such as an ion channel (KcsA) and a transporter protein (V-

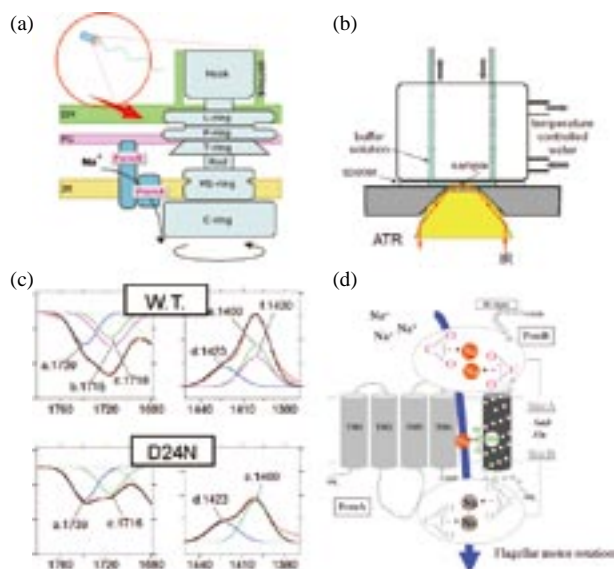


Figure 2. Sodium-ion binding induced difference FT-IR spectroscopy for a flagellar motor protein. (a) Schematic figure of supramolecular complex of flagellar motor. (b) A sample holder for perfusion-induced difference FT-IR spectroscopy. (c) COOH and COO⁻ vibrations observed upon dissociation and binding of sodium ions, respectively. One of them was assigned to Asp24. (d) The proposed mechanism for sodium-ion flux through the PomA/PomB complex.

ATPase), started before coming to IMS. It has been succeeded to measure the difference infrared spectra between the conditions of several types of ions and pH. Based on these spectra, the molecular mechanism of recognition and transportation of ions will be discussed in near future.

In Apr. 2010, a graduate student, Mr. Guo, joined our group and started to construct an ATR FT-IR measurement system with surface-enhanced technique. He has succeeded to make thin gold films by vapor deposition method and observed the AFM images. The surface enhancement of raman scattering from pyridine solution was confirmed by raman microscopy. In future, we will make a thin gold film on an ATR crystal, attach membrane proteins on the surface and measure the light and perfusion-induced difference FT-IR spectra.

3. FT-IR Studies for Revealing Molecular Mechanisms of Visual Rhodopsins

In our vision, rhodopsin works in the dim light and cone pigments in the daylight. The former is specialized for scotopic vision and the latter is for discriminating color.

We found that Thr118-OH group of bovine rhodopsin is utilized for an internal molecular probe to investigate protein fluctuation.²⁾ By monitoring a slow hydrogen/deuterium exchange (HDX) of the Thr118-OH group under native conditions and analyzing the data through the precise mathematical statistics, we proposed a quantitative two-step model in which the dark activation of rhodopsin is triggered by thermal isomerization of the retinal in a transiently opened conformation.

The red and green cone pigments from primate were heterologously expressed in HEK293 cells, purified by affinity chromatography, and then reconstituted in phosphatidylcholine (PC) liposomes. By using low-temperature FT-IR spectroscopy, the structural changes upon the retinal isomerization were analyzed and the molecular mechanism of red and green color discrimination was discussed.³⁾

Acknowledgements

We thank many collaborators, especially Profs. Hideki Kandori (Nagoya Institute of Technology), Michio Homma, Yuki Sudo (Nagoya University) and Hiroo Imai (Kyoto University). We also thank Prof. Yakushi's group for use of the vapor deposition apparatus and raman spectrometer. We also thank Prof. Urisu's group for use of AFM.

References

- 1) Y. Sudo, Y. Kitade, Y. Furutani, M. Kojima, S. Kojima, M. Homma and H. Kandori, *Biochemistry* **48**, 11699–11705 (2009).
- 2) V. A. Lórenz-Fonfría, Y. Furutani, T. Ota, K. Ido and H. Kandori, *J. Am. Chem. Soc.* **132**, 5693–5703 (2010).
- 3) K. Katayama, Y. Furutani, H. Imai and H. Kandori, *Angew. Chem., Int. Ed.* **49**, 891–894 (2010).

Heterogeneous Catalytic Systems for Organic Chemical Transformations

Department of Life and Coordination-Complex Molecular Science
Division of Complex Catalysis



UOZUMI, Yasuhiro
OSAKO, Takao
HAMASAKA, Go
ZHOU, Haifeng
BEPPU, Tomohiko
WATANABE, Toshihiro
KOBAYASHI, Noboru
MUTO, Tsubasa
TORII, Kaoru
TAZAWA, Aya
SASAKI, Tokiyo
FUKUSHIMA, Tomoko

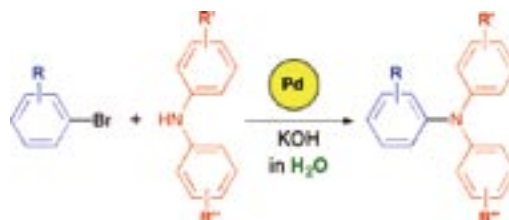
Professor
Assistant Professor
Post-Doctoral Fellow
Post-Doctoral Fellow
Graduate Student
Graduate Student
Graduate Student
Graduate Student
Technical Fellow
Technical Fellow
Secretary
Secretary

Various organic molecular transformations catalyzed by transition metals were achieved under heterogeneous conditions by use of amphiphilic resin-supported palladium complexes, palladium membrane-installed microchannel devices, or self-supported bipyridyl-palladium complexes which were designed and prepared by this research group. In particular, Buchwald-Hartwig reaction, Suzuki-Miyaura coupling, and aerobic alcohol oxidation, which were performed in water under heterogeneous conditions with high recyclability of the polymeric catalysts, are highlights among the achievements of the 2009–2010 period to approach what may be considered ideal chemical processes of next generation. Representative results are summarized hereunder.

1. Clean Synthesis of Triarylamines: Buchwald-Hartwig Reaction in Water with Amphiphilic Resin-Supported Palladium Complexes^{1,2)}

Catalytic aromatic amination was achieved in water under heterogeneous conditions by the use of immobilized palladium complexes coordinated with the amphiphilic polystyrene-poly(ethylene glycol) resin-supported di(*tert*-butyl)phosphine ligand. Aromatic amination of aryl halides with diphenylamine and *N,N*-double arylation of anilines with bromobenzene were

found to proceed in water with broad substrate tolerance to give the triarylamines in high yield with high recyclability of the polymeric catalyst beads. Very little palladium leached from the polymeric catalyst under the water-based reaction conditions to provide a green and clean (metal-uncontaminated) protocol for the preparation of triarylamines, including the optoelectronically active *N,N,N',N'*-tetraaryl-1,1'-biphenyl-4,4'-diamines (TPDs).

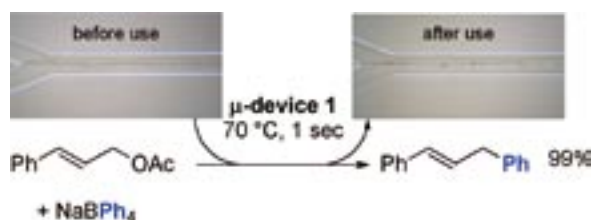


Scheme 1. Buchwald-Hartwig Reaction in Water with Amphiphilic Resin-Supported Palladium Complexes.

2. Palladium Membrane-Installed Microchannel Devices for Instantaneous Suzuki-Miyaura Cross-Coupling and Allylic Arylation^{3,4)}

Instantaneous catalytic carbon-carbon bond-forming reac-

tions were achieved in catalytic membrane-installed microchannel devices that have a polymeric palladium-complex membrane. The catalytic membrane-installed microchannel devices were provided inside the microchannels by means of coordinative and ionic molecular convection at the interface between the organic and aqueous phases flowing laminarily, in which both non-crosslinked linear polymer ligands and palladium species dissolved. The palladium-catalyzed Suzuki–Miyaura reaction of aryl, heteroaryl, and alkenyl halides with arylboronic acids and sodium tetraarylborates was performed with the catalytic membrane-installed microchannel devices to give quantitative yields of biaryls, heterobiaryls, and aryl alkenes within 5 s of residence time in the defined channel region. These microchannel devices were applied to the instantaneous allylic arylation reaction of allylic esters with arylboron reagents under microflow conditions to afford the corresponding coupling products within 1 s of residence time.



Scheme 2. Instantaneous Allylic Arylation with Palladium Membrane-Installed Microchannel Devices.

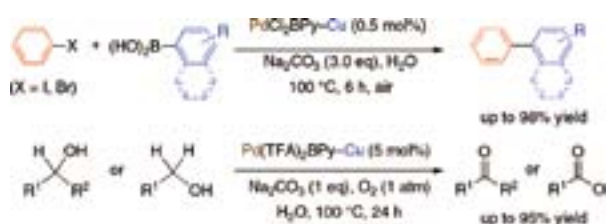
3. Suzuki–Miyaura Coupling and Aerobic Alcohol Oxidation in Water with Self-Supported Bipyridyl–Palladium Complexes^{5,6)}

Self-supported bipyridyl–palladium catalysts ($\text{PdX}_2\text{BPy–Cu}$) were developed *via* construction of metal–organic frame-

works (MOFs) of bipyridyl–palladium complexes bearing carboxylic groups and $\text{Cu}(\text{NO}_3)_2 \cdot 3\text{H}_2\text{O}$ (Scheme 3). The self-supported catalysts efficiently catalyzed the aerobic oxidation of benzylic alcohols and the Suzuki–Miyaura coupling of phenyl halides with arylboronic acids in water to give the corresponding products in high yield (Scheme 4). The catalysts were reused without a loss of catalytic activity.



Scheme 3. Preparation of Self-Supported Bipyridyl–Palladium Complexes *via* Construction of Metal–Organic Frameworks (MOFs).



Scheme 4. Suzuki–Miyaura Coupling and Aerobic Alcohol Oxidation in Water with Self-Supported Bipyridyl–Palladium Complexes.

References

- 1) Y. Hirai and Y. Uozumi, *Chem. Commun.* **46**, 1103–1105 (2010).
- 2) Y. Hirai and Y. Uozumi, *Chem. –Asian J.* **5**, 1788–1795 (2010) (Frontispiece Article).
- 3) Y. M. A. Yamada, T. Watanabe, K. Torii and Y. Uozumi, *Chem. Commun.* 5594–5596 (2009) (Hot Article).
- 4) Y. M. A. Yamada, T. Watanabe, T. Beppu, N. Fukuyama, K. Torii and Y. Uozumi, *Chem. –Eur. J.* **16**, 11311–11319 (2010).
- 5) T. Osako and Y. Uozumi, *Chem. Lett.* **38**, 902–903 (2009).
- 6) T. Osako and Y. Uozumi, *Heterocycles* **80**, 505–514 (2010).

Awards

UOZUMI, Yasuhiro; The 26th Inoue Prize for Science.
HAMASAKA, Go; CSJ Presentation Award 2010.

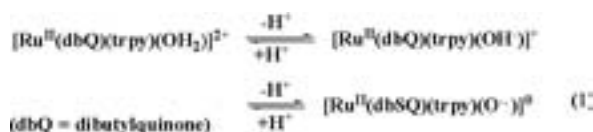
Synthesis of Metal Complexes Aiming at Storage and Release of Chemical Energy

Department of Life and Coordination-Complex Molecular Science
Division of Functional Coordination Chemistry



TANAKA, Koji	Professor
OHTSU, Hideki	Assistant Professor
KOBAYASHI, Katsuaki	IMS Research Assistant Professor
SUMANTA, Kumar	Post-Doctoral Fellow
BAI, Zhengshuai	Post-Doctoral Fellow
MIYAJI, Mariko	Post-Doctoral Fellow
TSUKAHARA, Yuhei	Graduate Student
DOYAMA, Yuko	Technical Fellow
YAMAGUCHI, Yumiko	Secretary
NOGAWA, Kyoko	Secretary

Metal complexes that have an ability to oxidize H₂ and alcohols at potentials more negative than reduction of dioxygen are feasible electrode catalysts in H₂/O₂ and alcohol/O₂ fuel cells. Electrochemical oxidation of Ru^{II}(polypyridyl)(OH₂) is accompanied by deprotonation to produce the correspondent Ru^{IV}=O and Ru^V=O complexes. Those high valent Ru=O complexes are expected for an application to electrode catalysts in fuel cells, since they have an ability to oxidize of some of organic molecules. However, intrinsic highly positive redox potentials for the generation of the active species does not meet a requirement to convert chemical energy of H₂ and alcohols to electricity. On the other hand, introduction of dioxolene ligands into Ru-aqua complexes results in spontaneous deprotonation of the aqua ligand, and unusual Ru-oxyl radical complexes are formed due to intra-molecular charge transfer from the resultant O²⁻ ligand to dioxolene (eq. 1). Oxyl radical complexes formed in eq. 1 are expected to have an ability of not only abstraction of hydrogen atom of C–H bonds of alcohols but also formation of oxygen–oxygen bond

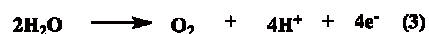
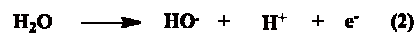


in the four-electron oxidation of water. Oxidations of alcohols and water under mild conditions would play the key role in the energy conversion to construct a sustainable society.

1. Substituents Dependent Capability of Bis(ruthenium-dioxolene)terpyridine Complexes toward Water Oxidation

Water splitting to H₂ and O₂ driven by visible light is an

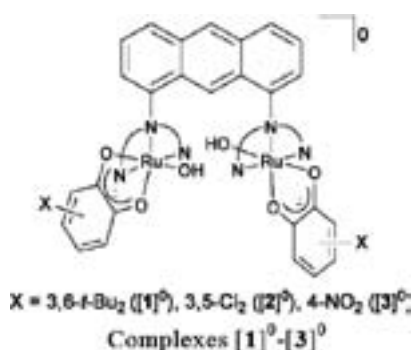
ultimate energy conversion from sunlight to a storable chemical energy. Water splitting using semiconductors under visible light irradiation has been well documented so far. Relatively low quantum efficiencies (~5%) in those reactions are ascribed to a reaction path through highly energetic one electron water oxidation that takes place at quite positive potentials (+2.31 V vs. NHE, pH 7, eq. 2). Accordingly, developments of efficient catalysts that have an ability to catalyze four-electron oxidation of water opens a door leading to an energetically sustainable society because four-electron water oxidation thermodynamically occurs at much more modest potentials (+0.815 V, eq. 3).



Recently, water oxidation using transition metal complexes has been intensively studied, though the reaction mechanism, especially the step of O–O bond formation from two water molecules, still remains unclear. Furthermore, Ce(IV) was used as an oxidant in most of water oxidation reactions. Taking into account that Ce(IV) is available as an oxidant only in very strong acidic aqueous solutions, electrochemical oxidation of water has various advantages not only to regulate the reaction conditions such as pH, applied potentials, and solvents but also to keep track of efficiencies and durability of catalysts by a change of catalytic currents during the reactions.

Dioxolene coordinated on metals take three redox states; quinone (q), semiquinone (sq), and catechol (cat). Among various metal-dioxolene complexes, ruthenium complexes in particular show strong interactions between Ru and dioxolene because of close energy levels of the dπ orbital of Ru to π and π* orbitals of dioxolene. Furthermore, three oxidation states of dioxolene are able to coordinate on Ru^{II}, Ru^{III} and Ru^{IV}, but

strict classification of those nine redox isomers (3×3) is practically impossible due to close energy levels of HOMO and LUMO energy levels of the metal and ligand. For example, the actual electronic structure of $[\text{Ru}(\text{OAc})(\text{dioxolene})(\text{trpy})]^0$ ($\text{trpy} = 2,2':4',2''\text{-terpyridine}$) gradually changes from the canonical $\text{Ru}^{\text{II}}(\text{sq})$ configuration to the $\text{Ru}^{\text{III}}(\text{cat})$ one with increasing electron withdrawing ability of dioxolene substituents. We have reported that a dinuclear ruthenium complex $[\text{Ru}_2(\text{OH})_2(3,6\text{-}t\text{-Bu}_2\text{q})_2(\text{btpyan})](\text{SbF}_6)_2$ ($[\mathbf{1}]^{2+}$, $3,6\text{-}t\text{-Bu}_2\text{q} = 3,6\text{-di-}t\text{-butyl-1,2-benzoquinone}$, $\text{btpyan} = 1,8\text{-bis}(2,2':6',2''\text{-terpyrid-4'-yl)anthracene}$) work as an excellent catalyst in the four-electron oxidation of water, since the electrochemical oxidation of water using an ITO electrode modified with $[\mathbf{1}](\text{SbF}_6)_2$ evolved large amounts of O_2 (33,500 turn-overs) at pH 4 (buffered) in H_2O . In the electrochemical oxidation of water catalyzed by $[\mathbf{1}]^{2+}$, redox reactions of dioxolene ligands play the central roles in not only the store of the electrons generated by proton dissociation of the hydroxyl group but also release of them to ITO electrode. However, the actual oxidation state of the Ru atom and dioxolene ligands in the catalytic cycle, and the process of the oxygen-oxygen bond formation prior to O_2 evolution still remain unclear. We, therefore, prepared bis(ruthenium-hydroxo) complexes having dichloro ($[\mathbf{2}]^0$) and NO_2 ($[\mathbf{3}]^0$) substituted dioxolene, and compared the redox behavior among $[\mathbf{1}]^0$, $[\mathbf{2}]^0$, and $[\mathbf{3}]^0$ to elucidate the role of dioxolene ligand in water oxidation.



The electronic structure of $[\mathbf{1}]^0$ is expressed by $[(\text{sq})\text{Ru}^{\text{II}}(\text{OH})(\text{HO})\text{Ru}^{\text{II}}(\text{sq})]^0$. The catalytic cycle of water oxidation by $[\mathbf{1}]^0$ is explained by the following stepwise reactions (i) two-electron oxidation of $[\mathbf{1}]^0$ produces $[(\text{q})\text{Ru}^{\text{II}}(\text{OH})(\text{HO})\text{Ru}^{\text{II}}(\text{q})]^{2+}$ ($[\mathbf{1}]^{2+}$), (ii) dissociation of protons coupled with electron transfer to q generates $[(\text{sq})\text{Ru}^{\text{II}}(\text{O}^{\cdot-})(^{\cdot-}\text{O})\text{Ru}^{\text{II}}(\text{sq})]^0$, (iii) coulomb repulsion between two $\text{O}^{\cdot-}$ ligands are removed by oxidation of sq, which facilitates to form O–O bond by a radical coupling reaction, (iv) an attack of water to a Ru atom is induced by oxidation of the complex, which cleaves one of the resultant Ru–O–O–Ru bond, (v) the second attack of water to another Ru atom release O_2 with regeneration of $[\mathbf{1}]^{2+}$. On the other hand, the electronic structures of $[\mathbf{2}]^0$ and $[\mathbf{3}]^0$ are

approximated by $[(\text{cat})\text{Ru}^{\text{III}}(\text{OH})(\text{HO})\text{Ru}^{\text{III}}(\text{cat})]^0$. Two-electron oxidation of the latter takes place on metal center to give $[(\text{cat})\text{Ru}^{\text{IV}}=\text{O}=\text{O}=\text{Ru}^{\text{IV}}(\text{cat})]^0$ rather than ligand centered oxidation affording $[(\text{sq})\text{Ru}^{\text{III}}(\text{OH})(\text{HO})\text{Ru}^{\text{III}}(\text{sq})]^{2+}$. It is considered that the O–O bond formation in $[(\text{cat})\text{Ru}^{\text{IV}}=\text{O}=\text{O}=\text{Ru}^{\text{IV}}(\text{cat})]^0$ is very hard due to the stability of the $(\text{cat})\text{Ru}^{\text{IV}}=\text{O}$ moiety. Indeed, the complexes $[\mathbf{2}]^0$ and $[\mathbf{3}]^0$ practically did not evolve O_2 under the electrolysis up to +2.20 V (vs. SCE) in H_2O .

2. A New Type of Electrochemical Oxidation of Alcohols Mediated with a Ruthenium-Dioxolene-Amine Complex in Neutral Water

The present society is maintained by combustion of tremendous amounts of fossil fuels and consumption of natural resources without regeneration of them. Global industrialization since 19 century inevitably has caused serious depletion of natural resources and environmental damages. As a result, energy conversion from natural energy to chemical one is believed as the top research area to build a sustainable society. Both H_2/O_2 and direct methanol (CH_3OH) fuel cells have the great feasibility as future energy sources. A key issue in practical uses of fuel cells is that only platinum or platinum-based alloys have been used as H_2 and CH_3OH oxidation electrodes. It is, therefore, highly desired to develop metal complexes that have an ability to oxidize H_2 and CH_3OH under mild conditions in place of platinum metal.

Aminyl radicals (NR_2^{\cdot}) that are known as reactive reaction intermediates abstract hydrogen atoms of various organic molecules. Some of those radicals are stabilized on metal complexes and successfully isolated. Recently, we have demonstrated that deprotonation of amino group of $\text{Ru}(\text{dioxolene})$ (amine) (dioxolene = 3,5-di-*tert*-butyl-1,2-benzoquinone (q), -semiquinonate (sq), and -catecholate (cat)) reversibly produces the correspondent aminyl radical complex due to an intra-molecular electron transfer between deprotonated amino group and dioxolene ligand. Although aminyl radical metal complexes hardly showed a catalytic activity for oxidation of organic molecules, two-electron oxidation of those complexes creates catalytic ability to oxidize alcohols. This fact has driven us to examine a potential application for electrocatalysts of oxidation of CH_3OH in aqueous conditions by considering smooth conversion between aminyl radical and amino groups on Ru. So, we examined the redox behavior of the $[\text{Ru}^{\text{II}}(\text{terpy})(\text{sq})(\text{NH}_3)]^+ / [\text{Ru}^{\text{II}}(\text{terpy})(\text{q})(\text{NH}_3)]^{2+}$ ($\text{terpy} = 2,2':6',2''\text{-terpyridine}$) couple (abbreviated as $[\text{Ru}^{\text{II}}(\text{sq})(\text{NH}_3)]^+ / [\text{Ru}^{\text{II}}(\text{q})(\text{NH}_3)]^{2+}$) in the absence and presence of a base in CH_3OH and in H_2O , and found an unprecedented two-electron oxidant character created by proton and electron loss of $[\text{Ru}^{\text{II}}(\text{q})(\text{NH}_3)]^{2+}$ in the oxidation of alcohols in neutral water.

Visiting Professors



Visiting Professor
NISHIHARA, Hiroshi (*from The University of Tokyo*)

Coordination Programming of Electro-Functional Materials

One goal of molecular electronics is to control electron conduction in molecular wires and networks by combining appropriate molecular units. To evaluate the total performance of the molecular wires, we are developing the construction of linear and branched metal complex oligomer and polymer wires by an interfacial stepwise coordination method and investigating electron conduction properties of internal molecular segments as well as the resistivity at the electrode-molecular wire junction. Also, the surface coordination programming of hetero molecular wires is being applied for development of cyanobacterial photosystem I (PSI)-based photosensors.



Visiting Associate Professor
UENO, Takafumi (*from Kyoto University*)

Novel Functional Nano Bio-Materials Based on Protein Assembly

Our research interests focus on the understanding, utilization, and design of protein assemblies that promote chemical reactions. We are developing strategies to functionalize natural protein assemblies as well as prepare artificial protein assemblies. This will expand the possibilities of our research into several emerging fields by bringing together the fields of organic chemistry, inorganic chemistry, biochemistry, molecular biology and structural biology.



Visiting Associate Professor
OYAMA, Dai (*from Fukushima University*)

Development of Highly Functionalized Transition Metal Complexes Based on Non-Innocent Ligands

Redox reactions are one of the most fundamental chemical reactions. Nature often utilizes redox-active organics in chemical transformations. Therefore, significant attention is currently focused on ligand-centered redox reactions in transition metal complexes.

We have investigated the synthesis and properties of the ruthenium complexes containing both pyridyl binding sites and azo, naphthyridine or quinone moieties which are closely related to biologically important molecules. In particular, we have studied on some important reaction systems such as multi-electron CO₂ reductions and H₂ evolution, based on proton-coupled electron transfer (PCET).